The Journal of Microbiology (2011) Vol. 49, No. 3, pp. 441-447
DOI 10.1007/s12275-011-0435-4

Sulfolipid Accumulation in *Mycobacterium tuberculosis* Disrupted in the *mce2* Operon[§]

Olivera Marjanovic[1]*, Anthony T. Iavarone[2], and Lee W. Riley[1]

[1]School of Public Health, [2]QB3/Chemistry Mass Spectrometry Facility, University of California, Berkeley, CA 94720, USA

(Received October 22, 2010 / Accepted January 20, 2011)

***Mycobacterium tuberculosis*, the causative agent of tuberculosis, has a lipid-rich cell wall that serves as an effective barrier against drugs and toxic host cell products, which may contribute to the organism's persistence in a host. *M. tuberculosis* contains four homologous operons called *mce (mce1-4)* that encode putative ABC transporters involved in lipid importation across the cell wall. Here, we analyzed the lipid composition of *M. tuberculosis* disrupted in the *mce2* operon. High resolution mass spectrometric and thin layer chromatographic analyses of the mutant's cell wall lipid extracts showed accumulation of SL-1 and SL_{1278} molecules. Radiographic quantitative analysis and densitometry revealed 2.9, 3.9 and 9.8-fold greater amount of [^{35}S] SL-1 in the *mce2* operon mutant compared to the wild type *M. tuberculosis* during the early/mid logarithmic, late logarithmic and stationary phase of growth in liquid broth, respectively. The amount of [^{35}S] SL_{1278} in the mutant also increased progressively over the same growth phases. The expression of the *mce2* operon genes in the wild type strain progressively increased from the logarithmic to the stationary phase of bacterial growth *in vitro,* which inversely correlated with the proportion of radiolabel incorporation into SL-1 and SL_{1278} at these phases. Since the *mce2* operon is regulated in wild type *M. tuberculosis*, its cell wall may undergo changes in SL-1 and SL_{1278} contents during a natural course of infection and this may serve as an important adaptive strategy for *M. tuberculosis* to maintain persistence in a host.**

***Keywords*:** mce operons, *M. tuberculosis*, sulfolipid-1, mass spectrometry, thin layer chromatography

Compared to most bacterial pathogens, *M. tuberculosis* possesses a distinct cell wall architecture, which accounts for its low permeability and thus for the organism's natural resistance to many common chemotherapeutic agents. It is estimated that nearly 60% of the dry weight of *M. tuberculosis*'s cell wall is comprised of lipids (Minnikin, 1982; Brennan and Draper, 1994; Daffe and Draper, 1998). This cell wall structure can be divided into two distinct barriers: the inner and the outer membrane barrier. The inner membrane barrier, referred to as the mycolyl-arabinogalactan-peptidoglycan complex, is composed of mycolic acids anchored to arabinogalactan, which is then linked to peptidoglycan (Minnikin, 1982). The outer membrane barrier is composed of an assortment of covalently bound mycolic acids and a vast array of "free" lipids, such as phthiocerol dimycoserosates (PDIM's), phenolic glycolipids (PGL's), trehalose containing glycolipids, and sulfolipids (SL) (Minnikin, 1982). Interspersed within this cell wall layer are proteins, phosphatidyl-*myo*-inositol mannosides (PIM's), lipomannan (LM), and lipoarabinomannan (LAM). PIM's, LM, and LAM are major glycolipids that are anchored to the plasma membrane through their phospatidyl-*myo*-inositol anchor and extend to the exterior of the cell wall (Besra and Brennan, 1997; Belanger and Inamine, 2000).

Mycobacterial lipids are involved in a variety of interactions with the host, including modulation of inflammatory response, mediation of bacterial trafficking within the macrophage, inhibition of phagocytosis and effector molecules of macrophages, and other processes that facilitate the long-term survival of *M. tuberculosis* in the infected host - a hallmark of this organism (Fratti *et al.*, 2003; Reed *et al.*, 2004; Vergne *et al.*, 2004; Geisel *et al.*, 2005; Rao *et al.*, 2005; Houben *et al.*, 2006). It is becoming increasingly recognized, however, that these cell wall lipid components are not static structures just designed to resist external toxic products, but that they undergo constant remodeling during a course of infection. These changes in the cell wall may constitute *M. tuberculosis*'s adaptive response to the stresses exerted by the infected host's immune cells that comprise the granulomas.

M. tuberculosis harbors 4 homologous copies of an operon called *mce* (*mce1-4*), which have been suggested to encode ATP-binding cassette (ABC) transporters, in particular lipid importer systems (Casali and Riley, 2007). Disruption of the *mce1* operon causes the *M. tuberculosis* mutant to become hypervirulent in mice (Shimono *et al.*, 2003). On the other hand, disruption of the other operons attenuates the mutants (Senaratne *et al.*, 2008; Marjanovic *et al.*, 2010). More recently, the *mce1* operon was shown to be involved in fatty acid or mycolic acid importation (Dunphy *et al.*, 2010), while *mce4* was suggested to encode a cholesterol import system (Pandey and Sassetti, 2008). These observations support the idea that these operons are involved in bacterial and host lipid processing during infection. Thus, in this study we set out to examine whether the *mce2* operon is also involved in lipid processing.

* For correspondence. E-mail: omarjanovic@berkeley.edu; Tel: +1-510-643-2949; Fax: +1-510-642-8250
§ Supplemental material for this article may be found at http://www.springer.com/content/120956

Materials and Methods

Generation of the *mce2* operon mutant strain

The construction of the *mce2* operon mutant was previously described (Marjanovic *et al.*, 2010). This mutant was constructed in a wild type H37Rv background by a strategy described by Parish and Stoker (Parish and Stoker, 2000). Briefly, following digestion with appropriate restriction enzymes the desired PCR products flanking the region targeted for deletion were subcloned into the p2NIL vector. Unmarked mutant was generated by a two-step counterselection process as previously described (Parish and Stoker, 2000). Southern Blot analysis was performed to confirm presence of the disruption of the operon sequence.

Growth and maintenance of Mycobacterial strains

M. tuberculosis strains were grown in Middlebrook 7H9 liquid medium (Difco, USA) supplemented with 10% albumin dextrose complex enrichment (Beckton-Dickinson, USA), 0.5% glycerol (Fisher Scientific, USA) and 0.05% Tween 80 (Fisher Scientific). Fresh bacterial stocks were thawed and grown to mid logarithmic phase, passaged and grown to a desired phase for lipid extraction.

Extraction of total lipids for thin layer chromatography and mass spectrometry

Extraction of lipids for thin layer chromatography (TLC) and mass spectrometry (MS) analysis was done according to the protocol described by Converse *et al*. (2003). All mycobacterial cultures were grown to a desired phase (mid logarithmic, stationary, or late stationary phase depending on experiment) in a 5% CO_2 humidified incubator at 37°C. An OD600 of mycobacterial cultures was recorded to ensure that the same number of organisms were present for each strain. Following this step, 8-10 ml cultures were centrifuged in 15 ml Falcon tubes at 3,000×g for 7 min, supernatants removed and lipids extracted from bacterial pellet as follows. Four mililiter of chloroform:methanol (2:1) was added to the pellet and the mixture transferred to scintillation vials (Fisher). This mixture was then vortexed for 2 h on a Genie 2 Vortex (Fisher) set on the lowest speed. This solvent extraction was then pelleted at 3,500×g. The supernatant containing the extracted lipids was then stored at -80°C until use.

Thin layer chromatography (TLC)

The following protocol was adapted from Dobson *et al*. (1985). Mycobacterial lipids were extracted as described above. They were first dried and concentrated under nitrogen gas. Resulting dried lipids were then resuspended in 200-400 µl of chloroform:methanol (2:1). These lipids were then spotted 1 cm from the bottom left edge of 5×7.5 cm Silica gel 60 F254 aluminum TLC plates (EMD, USA) with 5 µl Accupette Pipets (Dade Diagnostics, USA). The TLC chamber was equilibrated with filter paper and solvent. As shown in Supplementary data Table 1, the first listed solvent was used to perform one dimensional TLC, while two different solvents were used and applied in different directions to perform two dimensional TLC. TLC plates were developed with phosphomolybdic acid.

Mass spectrometry (MS)

Electrospray ionization mass spectrometry: Mass spectra were acquired in negative ion mode with a quadrupole time-of-flight (Q-Tof) mass spectrometer equipped with a Z-spray electrospray ionization (ESI) source (Q-Tof Premier™, Waters, USA). Ions were formed by syringe infusion ESI or by nanoESI. For syringe infusion ESI, sample solutions were withdrawn into a 250 µl Gastight® syringe (USA) and immediately infused into the ESI probe at flow rates of 5 to 10 µl/min using a syringe pump. Charged droplets of the sample solution were emitted from a stainless steel capillary (inner diameter 127 µm) with a nitrogen nebulizing gas flow of 800 L/h. For nanoESI, ions were formed from emitters made from borosilicate glass capillary tubes (1.0 mm o.d./0.78 mm i.d, Sutter Instruments, USA). These capillaries were pulled to a tip with an inner diameter of approximately 5 to 10 µm using a Flaming/Brown micropipette puller (Model P-87, Sutter). The spray was initiated by applying a potential of 0.5 to 1 kV to a Pt wire (0.127 mm diameter, Aldrich, USA) inserted into the nanoESI emitter to within approximately 2 mm of the tip. The flow rates were roughly 50 to 200 nl/min. No back pressure was used for nanoESI. Typical instrument parameters were as follows: capillary voltage 2 to 3 kV, sample cone 100 to 180 V, extraction cone 4 V, ion guide 3 V, source block temperature 80°C, desolvation (nebulizing) gas temperature 200°C, accelerating voltage into the argon-filled cell 4 V, first pumping stage pressure 1.4 mbar, ion transfer stage pressure 5×10^{-4} mbar, quadrupole analyzer pressure 1×10^{-5} mbar, argon-filled cell pressure 7×10^{-3} mbar, Tof analyzer pressure 8×10^{-7} mbar. No cone gas flow was used. For each sample, the sample cone and extraction cone voltages were adjusted to optimize signal for the ion(s) of interest, and the ESI capillary voltage was adjusted to maintain ion counts below the dead-time threshold (<0.1 ions per push) to prevent spectral distortion effects due to detector saturation. The Tof analyzer was operated in "V" mode. Under these conditions, a mass resolving power, R, of 1.0×10^{4} was routinely achieved, where $R=m/\Delta m_{50\%}$, m is the mass-to-charge ratio of an ion, and $\Delta m_{50\%}$ is the full width of the mass spectral peak at half-maximum height (Marshall *et al.*, 1998). This was more than sufficient to resolve the isotopic distributions of the singly and multiply charged ions measured in this study. Thus, an ion's mass and charge could be determined independently, i.e., an ion's charge state was determined from the reciprocal of the spacing between adjacent isotope peaks in the *m*/*z* spectrum. External mass calibration was performed with solutions of sodium formate or sodium iodide immediately prior to measuring samples. Mass spectra were processed with MassLynx software (version 4.1, Waters).

Radiometric analysis of sulfolipids

M. tuberculosis sulfolipids were labeled with [^{35}S] sulfate as previously described (Kumar *et al.*, 2007). Briefly, *M. tuberculosis* cultures were grown to OD600=0.9, 2.0, and 3.3 corresponding to mid logarithmic, late logarithmic, and stationary growth phases, respectively. Aliquots of 3-10 ml (depending on bacterial growth stage) of bacterial cultures (H37Rv and *mce2* operon mutant) were resuspended in 10 ml of PBS supplemented with 1 mg/ml sodium acetate and labeled with

Table 1. Fold difference in % radiolabel incorporation into SL^{-1} or SL_{1278} in Δ*mce2* operon relative to the wild type strain

Growth phase	SL^{-1}	SL_{1278}
OD_{600}=0.9	2.9 p=0.018	1.5 p=0.030
OD_{600}=2.0	3.9 p=0.022	3.4 p=0.043
OD_{600}=3.3	9.8 p=0.022	6.7 p=0.015

Quantification of % radiolabel incorporation was done with the ImageQuant 5.2 software. Results shown represent the average values from two independent experiments. Differences were considered significant when p≤0.05 as calculated by Student's t-test.

150 μCi of [^{35}S] sulfate for 18 h at 37°C. Cell pellets were washed, extracted with chloroform:methanol (2:1) and analyzed by TLC, eluting with water:isopropanol:ammonium hydroxide (1:6:1) as the developing solvent. Radioactivity was quantified by a phosphorimager followed by densitometry.

RNA preparation

DNA-free RNA was extracted from 5 ml of either middle logarithmic or stationary cultures of *M. tuberculosis* according to a standard Trizol RNA extraction protocol supplied by Invitrogen (Invitrogen, Life Technologies). Briefly, 5 ml of a culture was harvested during the exponential or stationary phase of bacterial growth by centrifugation at 3,500 rpm for 10 min. The cell pellet was resuspended in 1.5 ml of Trizol Reagent and transferred to a 2 ml screw-cap micro-centrifuge tube containing 0.1 mm diameter zirconium beads. Cells were disrupted with a FastPrep-24 bead-beater for 30 sec at a speed of 6±0 m/sec. The beating was done 3 times with 2 min ice incubations between beating runs. Total RNA was then extracted from the cells following the manufacturer's instructions.

Real-time quantitative PCR (RT-qPCR)

DNA-free RNA (500 ng) was mixed with 50 ng of random hexamer (Invitrogen) in 20 μl of final volume and reverse-transcribed to total cDNA with Superscript III reverse transcriptase (Invitrogen) following the manufacturer's recommendations. Identical reactions containing the same amount of RNA and lacking reverse transcriptase were also performed to confirm the absence of genomic DNA in all samples. The primers were designed to produce a 167-203 bp amplicon for each gene. Primer sets for each gene are shown below:

Primers for yrbE2A: Forward: tctaccggacatgcgtactg
Reverse: cagcaggatattgagcgtga
Primers for mce2A: Forward: agcggatttcctcacatgac
Reverse: gccagaatctgattgccatt
Primers for mce2F: Forward: tggtggtccttggttggtat
Reverse: gtagccattgtcgatgctca

Q-PCR reactions were performed with 25 ng of total cDNA previously generated and the Maxima SYBR Green/ROX qPCR Master Mix (2X) (Fermentas) according to manufacturer's instructions. Relative changes in the *mce2* operon gene expression in stationary relative to logarithmic phase of bacterial growth was calculated using the $2^{\wedge(-\Delta\Delta Ct)}$ method of analysis (Livak and Schmittgen, 2001).

Statistical analysis

Student's t-test was used to calculate statistical significance in fold difference in % radiolabel incorporation between wild type H37Rv and the *mce2* operon mutant strains during different phases of growth as well as fold difference in % radiolabel incorporation within the same strain at different phases of growth. Statistical significance in the fold difference in the expression levels of the *mce2* operon genes in the wild type strain at stationary relative to the exponential phase of growth was also calculated using the Student's t-test. Differences between different comparison groups were considered significant when $p \leq 0.05$. Values used in the Student's t-test calculation were the mean values of two different experiments each done in triplicates.

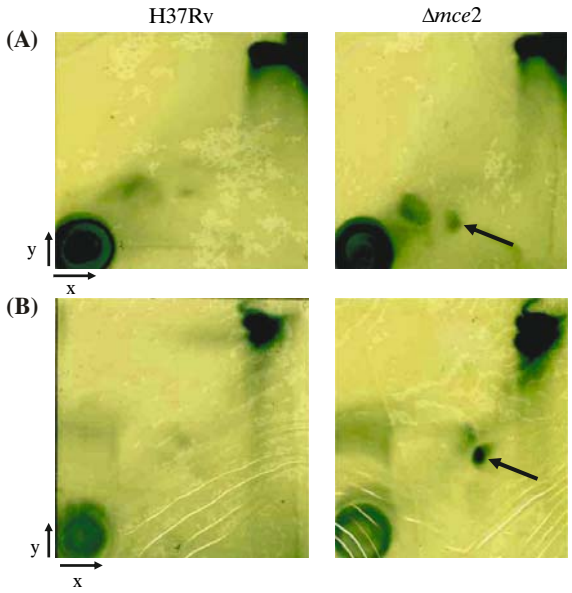

Fig. 1. Two dimensional TLC lipid profiles of total lipid extracts from the wild type *H37Rv* and *mce2* operon mutant bacteria (Δ*mce2*) grown to mid logarithmic phase. Solvent systems used were as follows: (A) petroleum ether:acetone (92:8, 3 runs) in X direction with toluene:acetone (95:5) in Y direction (B) chloroform:methanol:H_2O (100:14:0.8) in X direction with chloroform:acetone:methanol:H_2O (50:60:2.5:3) in Y direction. TLC plates were visualized by phosphomolybdic acid staining. Arrowheads point to the accumulating lipid present in the *mce2* operon mutant.

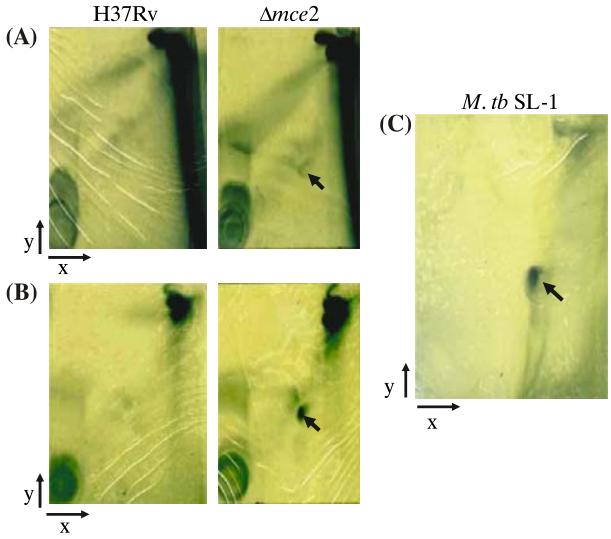

Fig. 2. Two dimensional TLC profiles of total lipid extracts from the wild type and the *mce2* operon mutant strains at different times of growth in liquid broth.The TLC's were run with chloroform:methanol:H_2O (100:14:08) in X direction and chloroform:acetone:methanol:H_2O (50:60:2.5:3) in Y direction using total lipid extracts from bacterial cultures grown for 21 days (A) or 41 days (B) in liquid broth. Two dimensional TLC profile of commercially purchased *M. tb* SL-1 is shown in (C). Total lipids were extracted, concentrated using nitrogen gas, and 10 μl of each bacterial strain extract run on the TLC plate. TLC plates were visualized by phosphomolybdic acid stain. Arrowheads point to the accumulating SL-1 present in the *mce2* operon mutant.

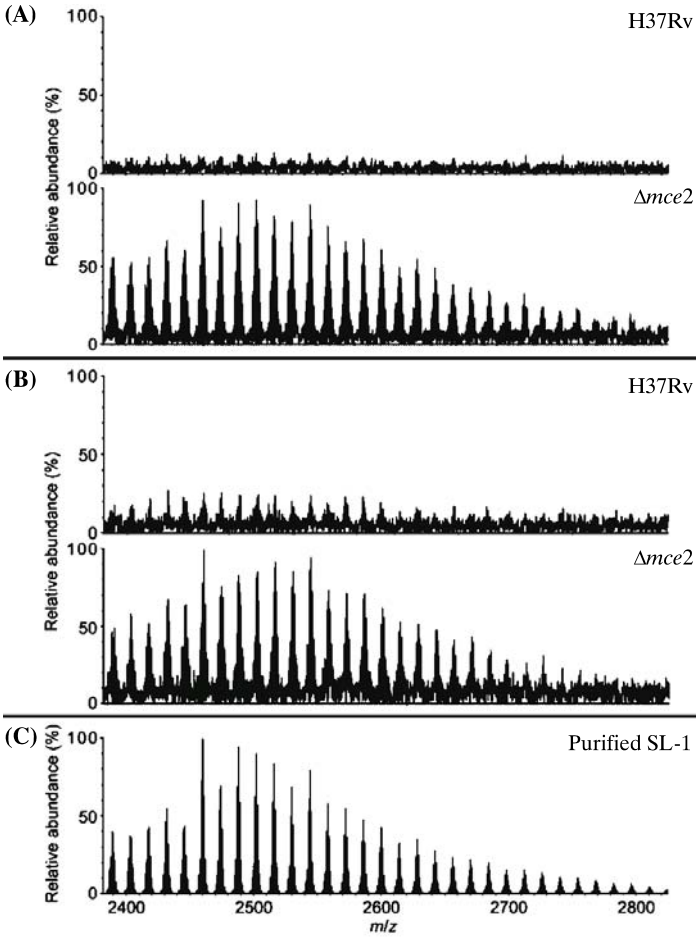

Fig. 3. MS analysis of expression of SL-1 in wild type H37Rv and *mce2* operon mutant strains. Total lipids were extracted from bacterial cultures grown to stationary phase (A) or late stationary phase (B) and analyzed by mass spectrometry. (C) Mass spectrum of SL-1 purified from *M. tuberculosis* (TimTec Inc.).

Results

Thin layer chromatography shows increased abundance of SL-1 in *mce2* operon mutant compared to wild type H37Rv bacteria

TLC was performed on lipid extracts run with a variety of solvent systems, which resolve the various lipid fractions present in the mycobacterial cell wall, as previously reported (Dobson *et al.*, 1985). Most notably, when the lipid extracts were run in the solvent system intended to resolve trehalose mycolates and sulfolipids, an increased amount of one lipid fraction in the *mce2* operon mutant lipid extract not present in that of wild type H37Rv was observed (Figs. 1A and B). Furthermore, this accumulation seemed to be time dependent. The longer the culture was grown in liquid broth, the more prominent this lipid spot became (Figs. 2A and B). Based on comparisons of these TLC results with those reported in the literature, this particular lipid spot corresponded to sulfolipid-1 molecule (SL-1) (structure of this molecule is shown in Supplementary data Fig. 1A). To further confirm this finding, we tested by TLC commercially available purified *M. tuberculosis* SL-1 (TimTec Inc.) alongside our *mce2* operon mutant lipid extract. We observed that purified SL-1 migrated to the same spot on the TLC plate as the lipid extracted from the *mce2* operon mutant bacterium (Fig. 2C). This finding led us to speculate that *mce2* operon mutant accumulates SL-1 in its cell wall, which prompted us to analyze this lipid fraction by mass spectrometry.

Mass spectrometry analysis of *mce2* operon mutant lipid profile shows increased abundance of SL-1 compared to H37Rv

We extracted total lipids from *mce2* operon mutant and *H37Rv* wild type strains and further analyzed these extracts by electrospray ionization MS. We were able to confirm our previous TLC results that showed SL-1 accumulation in the *mce2* operon mutant throughout different phases of growth *in vitro*, notably stationary and late stationary phases of bacterial growth (Figs. 3A and B, respectively). The MS profiles of our extracts reflect the characteristic SL-1 lipoforms previously established in the literature (Kumar *et al.*, 2007). Furthermore, we analyzed commercially available purified *M. tuberculosis*

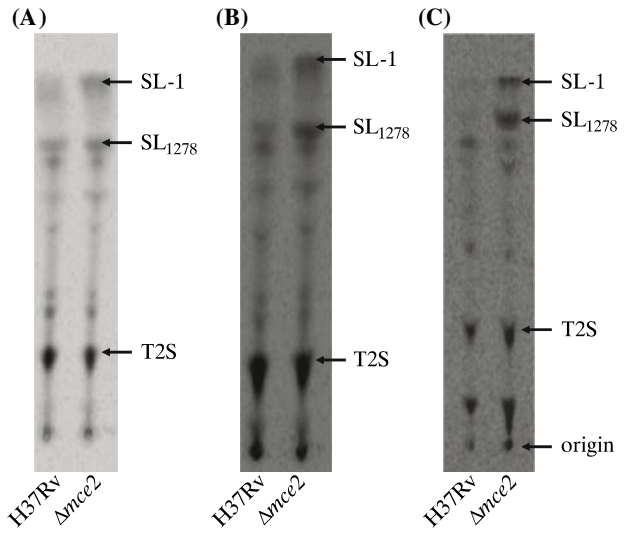

Fig. 4. *Mce2* operon mutant contains significantly higher levels of SL-1 and SL_{1278} than the wild type *H37Rv* strain. Bacterial cultures were grown to (A) early/mid logarithmic phase (B) late logarithmic phase and (C) stationary phase and their lipids were labeled by incubation with 150 μCi of [^{35}S] sulfate for 18 h. Total lipids were extracted and fractionated by TLC using H_2O:isopropanol:ammonium hydroxide (1:6:1) as the separating solvent. TLC plates were developed using phosphorimager and labeled lipid content in each strain quantified by densitometry. T2S (trehalose-2-sulfate) is an intermediate molecule in SL-1 biosynthetic pathway whose amount is comparable between the *mce2* operon mutant and wild type strains.

SL-1. As shown in Fig. 3C, SL-1 ions formed from the commercial, purified sample were observed in the same region of the mass spectrum as those formed from our experimental lipid extract.

Quantification of the SL-1 in H37Rv and the *mce2* operon mutant

To quantify the amount of SL-1 present in the wild type vs. the *mce2* operon mutant, we used [^{35}S] sodium sulfate as a tracer. Both wild type and the *mce2* operon mutant successfully incorporated ^{35}S into their lipid content within 18 h. The TLC lipid profiles of our extracts reflect the characteristic profiles of sulfated lipid molecules found in *M. tuberculosis* (Kumar *et al*., 2007). This method of lipid detection showed that the *mce2* operon mutant did not only accumulate SL-1 but that it also had a significantly higher amount of SL_{1278} molecule – a diacylated intermediate in the SL-1 biosynthetic pathway whose structure is shown in Supplementary data Fig. 1B (Converse *et al.*, 2003; Kumar *et al.*, 2007). More specifically, the [^{35}S] SL-1 abundance was 2.9-, 3.9-, and 9.8-fold greater

Table 2. RT-Q-PCR analysis of *mce2* operon genes in the stationary relative to the logarithmic phase of wild type bacterial growth

Gene	Fold difference in expression levels
yrbE2A	3.66±1.16[a]
mce2A	2.61±0.82[a]
mce2F	1.12±0.21

[a] Denotes statistical significance ($p \leq 0.05$) as calculated by Student's t-test.

Table 3. Fold difference in the % radiolabel incorporation into SL-1 and SL_{1278} in wild type strain in stationary relative to logarithmic phase of growth

Sulfated lipid	Logarithmic phase (% incorporation)	Stationary phase (% incorporation)	Fold difference
SL-1	4.33±1.3	0.13±0.03	34.1[a]
SL_{1278}	6.44±1.09	0.37±0.02	17.3[a]

[a] Denotes statistical significance ($p \leq 0.05$) as calculated by Student's t-test.

in the *mce2* operon mutant than in the wild type at early/mid logarithmic, late logarithmic and stationary phases of bacterial growth *in vitro* in liquid broth, respectively (Fig. 4 and Table 1). In addition, the levels of SL_{1278}, a molecule named after its observed mass, were 1.5-, 3.4-, and 6.7-fold greater in the *mce2* operon mutant than in the wild type bacterium at early/mid logarithmic phase, late logarithmic phase and stationary phase of bacterial growth, respectively (Fig. 4 and Table 1). We did not observe a significant difference in the amount of any other sulfated metabolites between the wild type and the *mce2* operon mutant strains.

Relative expression of the *mce2* operon genes in stationary relative to logarithmic phase of wild type bacterial growth

Increased and time dependant accumulation of sulfated lipids observed in the *mce2* operon mutant relative to the wild type strain seems to suggest that the expression of the *mce2* operon in the wild type may be greater in the stationary relative to logarithmic phase. The RT-qPCR analysis of RNA samples extracted at different phases of wild type bacterial growth showed that the expression of *mce2* operon genes in the stationary phase is significantly increased relative to their expression in the logarithmic phase (Table 2). Interestingly, the *mce2* operon gene expression was inversely correlated with the relative proportion of radiolabeled SL-1 and SL_{1278} detected in the wild type strain's lipid extracts at the same growth phases, suggesting that the activation of the operon may be associated with SL-1 and SL_{1278} catabolism (Table 3). We also quantified the amount of radiolabel present in these sulfated molecules in the *mce2* operon mutant and found that there is a decrease in radiolabel incorporation into sulfated molecules in stationary relative to logarithmic phase of growth (Supplementary data Table 2). This decrease was not as dramatic as in the wild type strain suggesting that there may be mechanisms other than *mce2* operon which are associated with SL-1 and SL_{1278} catabolism.

Discussion

The *mce* operons 1-4 of *M. tuberculosis* have been suggested to encode ABC transporters involved in lipid importation (Dassa and Bouige, 2001; Casali and Riley, 2007). *M. tuberculosis* disrupted in one of the *mce1* operon genes *fadD5* encoding fatty-acyl coenzyme A synthetase is diminished in growth in minimal medium supplied with only mycolic acids (Dunphy *et al.*, 2010). The *mce1* operon may play a role in recycling mycolic acids. The *mce4* operon was suggested to encode a putative cholesterol import system (Pandey and Sassetti, 2008). Taken together, these observations suggest that the *mce* operons regulate lipid processing in *M. tuberculosis*, perhaps

in response to its changing environment in the host. Here, we found that *M. tuberculosis* disrupted in the *mce2* operon showed significant changes in one of its major cell wall lipid components, namely sulfolipids. We suggest below how these changes may contribute to *M. tuberculosis*'s adaptive response to its host.

We found increased accumulation of SL-1 and SL_{1278} in the *mce2* operon mutant relative to the wild type strain. Unlike SL-1 which is found on the outer barrier of the cell wall, the location of SL_{1278}, believed to be a precursor of SL-1, remains unclear (Converse *et al.*, 2003; Kumar *et al.*, 2007). The accumulation of these molecules in the *mce2* operon mutant suggests a possible upregulation of the SL-1 biosynthetic pathway. However, analysis of relative expression levels of genes involved in the SL-1 biosynthetic pathway (Pks2, PapA1, and MmpL8) did not show a significant difference between the wild type and the *mce2* operon mutant strains (data not shown).

Alternatively, the *mce2* operon mutant may have a defect in the catabolism of SL-1. To date, not much is known about the catabolism of sulfated molecules in *M. tuberculosis*. Given that previous studies have implicated *mce* operons as being involved in lipid transport and metabolism (Casali and Riley, 2007; Pandey and Sassetti, 2008; Dunphy *et al.*, 2010), we propose that *mce2* operon may be involved in the transport and metabolism of sulfated lipids during particular stages of *M. tuberculosis* infection. Interestingly, in the wild type strain, the progressive increase in *mce2* operon gene expression from logarithmic to stationary growth phases inversely correlated with relative proportion of radiolabel incorporation into SL-1 and SL_{1278} at these phases (Tables 2 and 3). The increased radiolabel incorporation in these sulfolipids in the *mce2* operon mutant and the increased expression of the operon genes in the wild type strain with decreased radiolabel incorporation into these sulfolipids suggests that the activation of the operon facilitates the catabolism of these sulfated lipids.

SL-1 belongs to a family of sulfated trehalose esters with acyl groups, which was first recognized in the early 1960's when it was reported as a virulence factor of *M. tuberculosis* (Middlebrook *et al.*, 1959; Gangadharam *et al.*, 1963). Early *in vitro* studies showed that SL-1 stimulates release of superoxide (O_2^-) from human neutrophils and monocytes (Zhang *et al.*, 1988, 1991). At low concentrations (1-5 μg/ml) SL-1 can prime phagocytic cells for secondary challenge with mitogens (Zhang *et al.*, 1994). However, recent mouse studies with SL-1 mutant and wild type *M. tuberculosis* strains have shown no differences in infection outcomes (Converse *et al.*, 2003; Rousseau *et al.*, 2003). Okamoto and colleagues (2006) have reported that SL-1 can inhibit granuloma formation and macrophage TNF-α release caused by trehalose 6, 6'-dimycolate, a potent pro-inflammatory *M. tuberculosis* agent.

Our recent animal study with the *mce2* mutant has shown that the mutant is attenuated in mice and is diminished in its ability to elicit pro-inflammatory cytokine production in RAW macrophages (Marjanovic *et al.*, 2010). Lungs of mice infected with the mutant contained fewer granulomas than those of mice infected with the wild type H37Rv. Since we now know that the mutant accumulates SL-1, our animal study findings are consistent with the observations of Okamoto *et al.* (2006). That is, the accumulation of SL-1 may inhibit macrophage activation and hence reduce the granulomatous response.

Interestingly, the sulfated trehalose moiety of SL-1 is structurally similar to that of other sulfated carbohydrate molecules such as chondroitin sulfate and heparan sulfate that have been shown to have anti-inflammatory effects. Chondroitin sulfate induces immunological peripheral tolerance, a state characterized by accumulation of regulatory T cells responsible for curtailing excessive inflammation in tissues (Stacey *et al.*, 2003; Lin *et al.*, 2005). It is plausible to speculate that SL-1 may be playing a similar role during a natural course of *M. tuberculosis* infection.

Santangelo Mde and colleagues (2009) showed that the *mce2* operon is negatively regulated by *mce2R*. Therefore, during particular phases of infection, when the *mce2* operon becomes repressed, SL-1 may indeed accumulate in the cell wall of wild type *M. tuberculosis.* That is, the accumulation of SL-1 may be part of a natural physiologic state of *M. tuberculosis* during a course of infection. The host immune cells may become less responsive to this population of bacilli expressing large amounts of SL-1. That is, SL-1 may induce a form of immunological tolerance, which not only protects the bacteria but also preserves the integrity of host tissue. The preservation of host tissue integrity is important for *M. tuberculosis*, which must persist in its host. Thus, we propose that *M. tuberculosis*, via the *mce2* operon, remodels its cell wall architecture in response to changes in host immune response over the course of an infection to promote the bacteria's long-term survival.

Acknowledgements

We thank Nicola Casali, Sally A. Cantrell, Michael D. Leavell, and Eva Raphael for helpful discussions. This project was funded by an NIH/NIAID grant (R01AI073204).

References

Belanger, A.E. and J.M. Inamine. 2000. Genetics of Cell Wall Biosynthesis, pp. 191-202. *In* G.F. Hartfull and W.R.J. Jacobs (eds.), Molecular Genetics of Mycobacteria. American Society of Microbiology, Washington, DC, USA.

Besra, G.S. and P.J. Brennan. 1997. The mycobacterial cell wall: biosynthesis of arabinogalactan and lipoarabinomannan. *Biochem. Soc. Trans.* 25, 845-850.

Brennan, P.J. and P. Draper. 1994. Ultrastructure of *Mycobacterium tuberculosis*, pp. 271-306. *In* B.R. Bloom (ed.), Tuberculosis: Pathogenesis, Protection and Control. ASM Press, Washington, DC, USA.

Casali, N. and L.W. Riley. 2007. A phylogenomic analysis of the Actinomycetales *mce* operons. *BMC Genomics* 8, 60.

Converse, S.E., J.D. Mougous, M.D. Leavell, J.A. Leary, C.R. Bertozzi, and J.S. Cox. 2003. MmpL8 is required for sulfolipid-1 biosynthesis and *Mycobacterium tuberculosis* virulence. *Proc. Natl. Acad. Sci. USA* 100, 6121-6126.

Daffe, M. and P. Draper. 1998. The envelope layers of mycobacteria with reference to their pathogenicity. *Adv. Microb. Physiol.* 39, 131-203.

Dassa, E. and P. Bouige. 2001. The ABC of ABCS: a phylogenetic and functional classification of ABC systems in living organisms. *Res. Microbiol.* 152, 211-229.

Dobson, G., D.E. Minnikin, S.M. Minnikin, J.H. Parlett, M. Goodfellow, M. Ridell, and M. Magnusson. 1985. Systematic

analysis of complex mycobacterial lipids, pp. 237-265. *In* M. Goodfellow and D.E. Minnikin (eds.), Chemical Methods in Bacterial Systematics. Academic Press, London, UK.

Dunphy, K.Y., R.H. Senaratne, M. Masuzawa, L.V. Kendall, and L.W. Riley. 2010. Attenuation of *Mycobacterium tuberculosis* functionally disrupted in a fatty acyl-coenzyme A synthetase gene *fadD5*. *J. Infect. Dis.* 201, 1232-1239.

Fratti, R.A., J. Chua, I. Vergne, and V. Deretic. 2003. *Mycobacterium tuberculosis* glycosylated phosphatidylinositol causes phagosome maturation arrest. *Proc. Natl. Acad. Sci. USA* 100, 5437-5442.

Gangadharam, P.R., M.L. Cohn, and G. Middlebrook. 1963. Infectivity, pathogenicity and sulpholipid fraction of some Indian and British strains of tubercle Bacilli. *Tubercle* 44, 452-455.

Geisel, R.E., K. Sakamoto, D.G. Russell, and E.R. Rhoades. 2005. *In vivo* activity of released cell wall lipids of *Mycobacterium bovis* bacillus Calmette-Guerin is due principally to trehalose mycolates. *J. Immunol.* 174, 5007-5015.

Houben, E.N., L. Nguyen, and J. Pieters. 2006. Interaction of pathogenic mycobacteria with the host immune system. *Curr. Opin. Microbiol.* 9, 76-85.

Kumar, P., M.W. Schelle, M. Jain, F.L. Lin, C.J. Petzold, M.D. Leavell, J.A. Leary, J.S. Cox, and C.R. Bertozzi. 2007. PapA1 and PapA2 are acyltransferases essential for the biosynthesis of the *Mycobacterium tuberculosis* virulence factor sulfolipid-1. *Proc. Natl. Acad. Sci. USA* 104, 11221-11226.

Lin, H.H., D.E. Faunce, M. Stacey, A. Terajewicz, T. Nakamura, J. Zhang-Hoover, M. Kerley, M.L. Mucenski, S. Gordon, and J. Stein-Streilein. 2005. The macrophage F4/80 receptor is required for the induction of antigen-specific efferent regulatory T cells in peripheral tolerance. *J. Exp. Med.* 201, 1615-1625.

Livak, K.J. and T.D. Schmittgen. 2001. Analysis of relative gene expression data using real-time quantitative PCR and the 2(-Delta Delta C(T)) method. *Methods* 25, 402-408.

Marjanovic, O., T. Miyata, A. Goodridge, L.V. Kendall, and L.W. Riley. 2010. *Mce2* operon mutant strain of *Mycobacterium tuberculosis* is attenuated in C57BL/6 mice. *Tuberculosis* 90, 50-56.

Marshall, A.G., C.L. Hendrickson, and G.S. Jackson. 1998. Mass spectrom. *Review* 17, 1-35.

Middlebrook, G., C.M. Coleman, and W.B. Schaefer. 1959. Sulfolipid from virulent tubercle Bacilli. *Proc. Natl. Acad. Sci. USA* 45, 1801-1804.

Minnikin, D.E. 1982. Lipids: complex lipids, their chemistry, biosynthesis and roles, pp. 95-184. *In* C. Ratledge and J. Stanford (eds.), The Biology of Mycobacteria. Academic Press, Ltd., London, UK.

Okamoto, Y., Y. Fujita, T. Naka, M. Hirai, I. Tomiyasu, and I. Yano. 2006. Mycobacterial sulfolipid shows a virulence by inhibiting cord factor induced granuloma formation and TNF-alpha release. *Microb. Pathog.* 40, 245-253.

Pandey, A.K. and C.M. Sassetti. 2008. *Mycobacterial persistence* requires the utilization of host cholesterol. *Proc. Natl. Acad. Sci. USA* 105, 4376-4380.

Parish, T. and N.G. Stoker. 2000. Use of a flexible cassette method to generate a double unmarked *Mycobacterium tuberculosis* tlyA plcABC mutant by gene replacement. *Microbiology* 146, 1969-1975.

Rao, V., N. Fujiwara, S.A. Porcelli, and M.S. Glickman. 2005. *Mycobacterium tuberculosis* controls host innate immune activation through cyclopropane modification of a glycolipid effector molecule. *J. Exp. Med.* 201, 535-543.

Reed, M.B., P. Domenech, C. Manca, H. Su, A.K. Barczak, B.N. Kreiswirth, G. Kaplan, and C.E. Barry, 3rd. 2004. A glycolipid of hypervirulent tuberculosis strains that inhibits the innate immune response. *Nature* 431, 84-87.

Rousseau, C., O.C. Turner, E. Rush, Y. Bordat, T.D. Sirakova, P.E. Kolattukudy, S. Ritter, I.M. Orme, B. Gicquel, and M. Jackson. 2003. Sulfolipid deficiency does not affect the virulence of *Mycobacterium tuberculosis* H37Rv in mice and guinea pigs. *Infect. Immun.* 71, 4684-4690.

Santangelo Mde, L., F. Blanco, E. Campos, M. Soria, M.V. Bianco, L. Klepp, A. Alito, O. Zabal, A. Cataldi, and F. Bigi. 2009. Mce2R from *Mycobacterium tuberculosis* represses the expression of the *mce2* operon. *Tuberculosis* 89, 22-28.

Senaratne, R.H., B. Sidders, P. Sequeira, G. Saunders, K. Dunphy, O. Marjanovic, J.R. Reader, and *et al*. 2008. *Mycobacterium tuberculosis* strains disrupted in *mce3* and *mce4* operons are attenuated in mice. *J. Med. Microbiol.* 57, 164-170.

Shimono, N., L. Morici, N. Casali, S. Cantrell, B. Sidders, S. Ehrt, and L.W. Riley. 2003. Hypervirulent mutant of *Mycobacterium tuberculosis* resulting from disruption of the *mce1* operon. *Proc. Natl. Acad. Sci. USA* 100, 15918-15923.

Stacey, M., G.W. Chang, J.Q. Davies, M.J. Kwakkenbos, R.D. Sanderson, J. Hamann, S. Gordon, and H.H. Lin. 2003. The epidermal growth factor-like domains of the human EMR2 receptor mediate cell attachment through chondroitin sulfate glycosaminoglycans. *Blood* 102, 2916-2924.

Vergne, I., J. Chua, S.B. Singh, and V. Deretic. 2004. Cell biology of *Mycobacterium tuberculosis* phagosome. *Annu. Rev. Cell. Dev. Biol.* 20, 367-394.

Zhang, L., D. English, and B.R. Andersen. 1991. Activation of human neutrophils by *Mycobacterium tuberculosis*-derived sulfolipid-1. *J. Immunol.* 146, 2730-2736.

Zhang, L., J.C. Gay, D. English, and B.R. Andersen. 1994. Neutrophil priming mechanisms of sulfolipid-I and N-formyl-methionyl-leucyl-phenylalanine. *J. Biomed. Sci.* 1, 253-262.

Zhang, L., M.B. Goren, T.J. Holzer, and B.R. Andersen. 1988. Effect of *Mycobacterium tuberculosis*-derived sulfolipid I on human phagocytic cells. *Infect. Immun.* 56, 2876-2883.